

# PL/EL IMAGE ANALYSIS OF RADIATION DETERIORATION IN TRIPLE-JUNCTION SOLAR CELLS

Yuki Kobayashi\*<sup>1</sup>, Mitsuru Imaizumi<sup>1</sup>, Shirou Kawakita<sup>1</sup> and Masato Takahashi<sup>1</sup>

<sup>1</sup> Japan Aerospace Exploration Agency (JAXA), Japan

\*Email: kobayashi.yuki@jaxa.jp

Keyword(s): Triple-junction solar cell, photoluminescence, electroluminescence, radiation degradation

## Abstract

We are developing a compact and lightweight automated inspection system of solar panel that can acquire photoluminescence (PL) and electroluminescence (EL) images of InGaP/GaAs/Ge triple-junction solar cells simultaneously (PL and EL images acquisition system; PEAS). We would like to contribute to reduce the burden for visual checking inspections of solar cells on solar panel and improve inspection accuracy by applying PL/EL observation to solar panels. For that purpose we consider that building knowledge-based PL/EL images is necessary. Currently, we are studying the interrelation between environmental test effects and PL/EL images. In this paper, we evaluate correlation between radiation degradation of triple-junction solar cells and change in PL/EL images.

## 1. Introduction

To enable anyone to check the mechanical defects and electro-current constriction spots of solar cells or solar panels easily and quickly through observation of Photoluminescence (PL) and electroluminescence (EL) images, we are developing an automated inspection system for solar panels, which simultaneously takes PL and EL images of triple-junction solar cells on a panel.

PL and EL observations are highly sensitive methods for examining impurities, a variety of imperfections such as crystal defects and mechanical cracks within materials, and are extremely effective methods for assessing solar cell imperfections. Two-dimensional PL and EL image observation allows us direct visual evaluation with the naked eye. Although the EL method requires an external power source to supply current, it has the advantage of being able to quickly detect solar cell output power failures, which is shunting, since such a shunting spot is detected as a bright point caused by currents concentrating there. On the other hand, the PL method is advantageous in that evaluations can be conducted in a completely noncontact manner; therefore, it can be applied when we cannot apply electric bias or current to a subject solar cell.

The imperfections in PL and EL images on solar cells can be grouped into two cases substantially: One is native defects originated from epitaxial growth such as crystal defects in the layers, and the other is mechanical defects caused by extrinsic factors such as mechanical stress during coverglass/interconnector/cell (CIC) assembly, lay-down processes, or environmental tests. PL and EL images exhibit a variety of contrast patterns in a solar cell regardless of whether the origin of the pattern influences solar cell output. Thus, it is necessary for us to determine whether the observed imperfections on PL/EL images of solar cells or solar paddles will eventually cause electrical power loss. The imaging of PL and EL can show, in a simple and visual manner, the patterns reflecting various properties of solar cells, regardless of whether or not the source of the observed luminescence pattern has influence on the output power of solar cells. Therefore, it is necessary for us to figure out what the image observed is to be ascribed to and whether or not that is the image to be called into account in evaluating the panels of the solar cells. For that reason, we think it is needed to construct a knowledge base about the luminescence patterns of PL and EL. Currently we are conducting, in preparation for the construction of the knowledge base, the examination on the changes in the luminescence patterns before and after the environmental load test.

In the following proceedings we explain the automated evaluation device for PL and EL and report on the radiation impact of the solar cell panels, which have a characteristic leak path.

## 2. PL and EL Image Acquisition System (PEAS)

We are currently developing an automated inspection system using PL and EL images for solar panels composed of InGaP/GaAs/Ge triple-junction cells. Fig. 1 depicts a schematic of an acquiring unit of the PL and EL images acquisition system (PEAS). The PEAS can simultaneously acquire PL and/or EL image in a scan. The image acquiring unit of PEAS consists of two charge-coupled device (CCD) cameras equipped with band-pass filters suitable for observing luminescence from InGaP and GaAs subcells in a triple-junction solar cell, and a pair of light-emitting diode (LED) units as excitation light sources for the PL; a unit consists of two types of LEDs, namely, one for excitation of InGaP subcells, the other for GaAs subcells. Two LED units are mounted with certain angle against the solar panel to achieve the uniformity of light intensity. The LEDs were selected for

excitation as they have peak wavelengths ( $\lambda_D$ ) and half width suited for the EQE of each subcell. Band-pass filters are also selected in the same way as they have transparent wavelength bands suited for each LED and PL from each subcell.

A simplified schematic of the system is shown in Fig. 2. The system consists of an image acquiring XY-stage including an acquiring unit on the Z-stage, an XYZ-stage control unit, and a mobile personal computer (PC). A solar panel is set on the fixture frame. The PC allows us to control the XYZ-stage and the two CCD cameras to obtain the EL and PL image on the solar panel. Communications to those devices are made by original software written in the LabVIEW program (National Instruments, Inc.). The system can obtain three images of a triple-junction cell in a scan. The four images are EL images of InGaP top and GaAs middle subcells, and PL images of either subcell.

Shown in Fig.3 is a picture of a X- and Y-axis extendable PEAS (XY-PEAS). XY-PEAS is suitable for a diagnosis of larger solar panels. XY-PEAS consist of the main-PEAS, extendable Y-axis unit and X-axis rail unit. Each unit can be separated. And the each units can be detached easily for transport and reconstructed easily. The maximum scan length along the Y-axis is extended to 1.8 m. The minimum footprint is around 1.2 m  $\times$  1 m, including the rail unit. The rail unit can be extended every 1.2 m. This makes it possible to expand the observation area to accommodate any size of solar panel. The control unit of XY-PEAS was improved from three axes (X-, Y- and Z-axis) to five axes (with the addition of the extended X- and Y-axis). XY-PEAS can be driven automatically along the five axes via the PC.

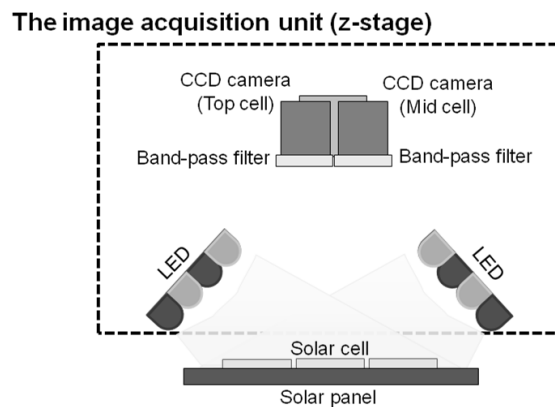


Figure 1. Schematic of the acquiring unit of the PL and EL image acquiring unit

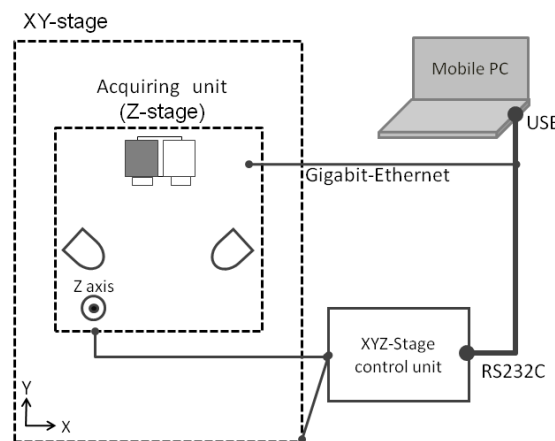


Figure 2. Simplified schematic of the PL and EL image acquiring system (main-PEAS)

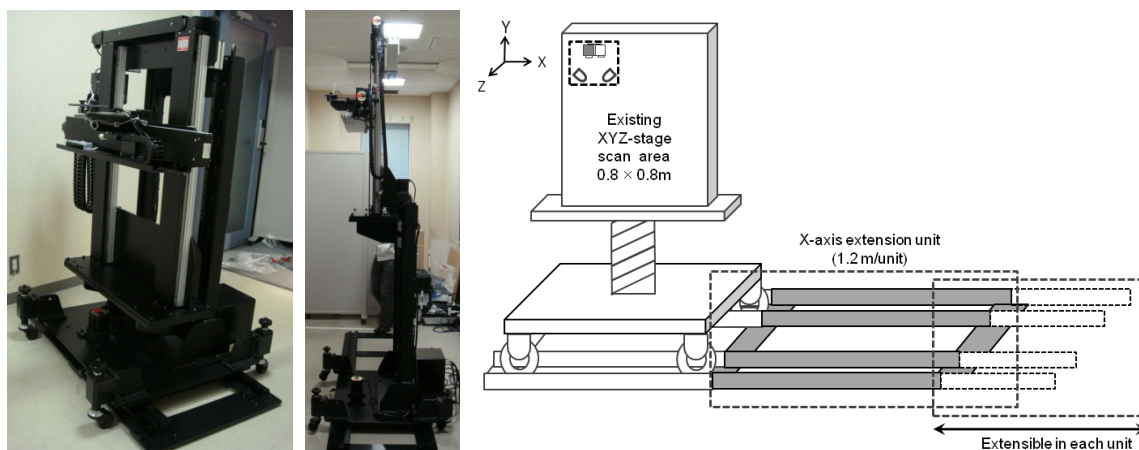


Figure 3. Schematic of X- and Y-axis extendable PEAS (XY-PEAS)

### 3. Various PL and EL Evaluations for Knowledge-base construction

#### 3.1 Experiment

We have used the InGaP/GaAs/Ge triple-junction solar cells with cover glass  $4 \times 8\text{cm}$  as samples. PL / EL images were evaluated. The 1MeV electron beam irradiation test was carried out regarding 3J cells (#1) that do not have a special light emission pattern both on the top and mid layer and 3J cells (#2) that have dark spots on the top layer. The dose amount was  $1 \times 10^{13}$  and  $1 \times 10^{15} \text{ e}^-/\text{cm}^2$ . PL / EL imaging evaluation was conducted before the electron beam irradiation and after the irradiation at each dose. In addition, we have evaluated the light IV characteristics and spectral sensitivity characteristics before the irradiation and after the irradiation at  $1 \times 10^{15} \text{ e}^-/\text{cm}^2$ .

#### 3.2 Result & discussion

Table 1 shows PL/EL image of before and after electron beam irradiation ( $1 \text{ MeV}$  electron,  $1 \times 10^{13} \text{ e}^-/\text{cm}^2$ ) of sample #1 and #2. Table 1 indicates that the cell of #2 has a typical dark spot in the top layer and the image of PL/EL in the middle layer shows a tiny dark spot and two small bright ones make a large dark spot. (Recognized as a singular and specific spot.) While the cell of #1 that does not possess a large dark spot decreases the overall emission intensity, not a substantial change of relative distribution has been found. On the other hand, #2 cell that has a typical dark spot in the top layer does not show a big relative change of emission distribution but in the middle layer a substantial change of emission intensity and a relative change of emission distribution with the singular and specific spot have been noticed.

Table 1 Acquired PL and EL images of top and middle subcells of before and after the irradiation.

	#1		#2	
	BOL	1MeV, $1 \times 10^{13} \text{ e}^-/\text{cm}^2$	BOL	1MeV, $1 \times 10^{13} \text{ e}^-/\text{cm}^2$
PL image of InGaP		 Exposure time: 1.3*BOL		 Exposure time: BOL
EL image of InGaP (I=1/2Isc)		 Exposure time: 1.2*BOL		 Exposure time: 1.3*BOL
PL image of GaAs		 Exposure time: 5.2*BOL		 Exposure time: 5*BOL
EL image of GaAs (I=1/2Isc)		 Exposure time: 8.6*BOL		 Exposure time: 3*BOL

Fig. 4 shows The light IV characteristics of #1 and #2 before and after the irradiation of 1MeV electron beams ( $1 \times 10^{15} \text{ e}^-/\text{cm}^2$ ). Comparison of the beginning of life (BOL) characteristics in Fig. 4 indicates that while both the short circuit current ( $I_{sc}$ ) and open circuit voltage ( $V_{oc}$ ) decreased, the presence of dark spots in the cells did not lead to any significant performance deterioration.

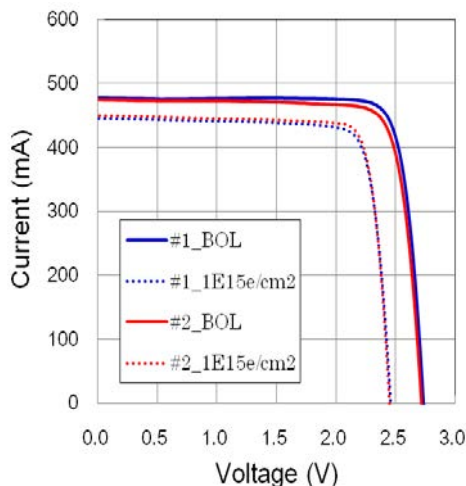


Fig.4 The light IV characteristics of #1 and #2 cells before and after the irradiation. The fluence is  $1 \times 10^{15} \text{ e}^-/\text{cm}^2$ .

Table 2 Performance parameters of #1 and #2 cells before and after the irradiation.

	Case	Isc(mA)	Remaining factor of Isc	Voc(V)	Remaining factor of Voc	FF(%)
#1	BOL	478	-	2.74	-	84.01
	EOL 1MeV, $1 \times 10^{15} \text{ e}^-/\text{cm}^2$	446	0.934	2.46	0.898	82.47
#2	BOL	468	-	2.72	-	82.26
	1MeV, $1 \times 10^{15} \text{ e}^-/\text{cm}^2$	449	0.959	2.45	0.904	83.72

#### 4. SUMMARY

When 1 MeV electron beams with irradiation energy of  $1 \times 10^{13}$  and  $1 \times 10^{15} \text{ e}^-/\text{cm}^2$  were irradiated on 3J cells (CIC), the electron beam irradiation caused changes in PL/EL emission intensity in the mid cell of a 3J cell having dark spots with a particular characteristic. Examinations of electrical properties and spectral responses suggested no significant performance deterioration regardless of whether the cells had dark spots due to the irradiation of 1 MeV electron beam.

Since results in this research is based on a small number of observations, we plan to repeat the experiments in future. Further, we plan to conduct investigations on the effects of defects other than dark spots.

#### Acknowledgments

We would like to thank to Dr. Kazunori Shimazaki of JAXA, Mr. Jiro Harada and Mr. Yoichi Hagiwara of Advanced Engineering Services Co., Ltd,